Evidence for Ion Chain Mechanism of the Nonlinear Charge Transport of Hydrophobic Ions Across Lipid Bilayers

Kai Sun and David Mauzerall
The Rockefeller University, New York, New York 10021 USA

ABSTRACT The conductivity across a lipid bilayer by tetraphenylborate anion is increased 10-fold on the photoformation of lipophilic porphyrin cations. The cations alone have negligible conductivity. This nonlinear photogenerated increase of ion conductivity is termed the photogating effect. Substitution of H by Cl in the *para* position of tetraphenylborate leads to a 100-fold enhancement of conductivity, whereas the dark conductivities for this and other substituted borates are the same. Moreover, the halo-substituted borates show a large enhancement of conductivity in the low concentration range (10^{-8} M), whereas that of tetraphenylborate is small and space charge is negligible. The enhanced ion conductivity has great structural sensitivity to the structure of the anion, the cation, and the lipid, whereas the partition coefficient of all the borates and the concentration of photoformed cations are only slightly affected. The photogated ion transport has a twofold larger activation energy than transport in the dark. Time-resolved photocurrents and voltages demonstrate that the translocation rate of the porphyrin cation is also enhanced 100-fold by the Cl-borate anion but only 10-fold by the H-borate anion. For these reasons the nonlinear gating effect cannot be explained by electrostatics alone, but requires an ion chain or ion aggregate mechanism. Kinetic modeling of the photoinduced current with a mixed cation-anion ion chain can fit the data well. The photogating effect allows the direct study of ion interactions within the bilayer.

INTRODUCTION

The lipid bilayer is the very definition of a cell. The formation of membrane potentials and transmembrane ion transport are principal properties of biological membranes. The study of these basic properties in lipid bilayers has attracted much research (McLaughlin, 1977; Läuger et al., 1981; Honig et al., 1986). In most of the published studies attention has been paid to the electrostatic properties and the ion behavior at membrane-water interfaces (McLaughlin, 1977, 1989; Huber and Ramberg, 1981; Cevc, 1990) and to the translocation and distribution of a single kind of ion in the bilayer (Andersen and Fuchs, 1975; Benz et al., 1976; Läuger et al., 1981). In contrast, there are few studies (Liberman and Topaly, 1969; Drain et al., 1989; Drain and Mauzerall, 1992; Mauzerall and Drain, 1992) on the ion interactions, cooperative translocation, and related electrostatics of different kinds of ions inside the lipid membrane because of a lack of efficient probing methods. Hydrophobic ions in lipid bilayers have been used to study fundamentals of transmembrane charge transport to avoid the ion complexing steps of ion carriers (Läuger et al., 1981). The translocation of a single kind of ion has been examined by monitoring the current relaxations after an applied voltage jump (Ketterer et al., 1971; Andersen and Fuchs, 1975) or by monitoring the voltage relaxations after an applied charge pulse across lipid membranes (Benz et al., 1976; Läuger et al., 1981). Spin-label techniques with lipophilic ions (Cafiso and Hubbell, 1981; Perkins and Cafiso, 1987) also offer a way to probe the internal properties of the bilayer. Because this method largely measures the static partitioning of hydrophobic ions between the membrane and aqueous phases, however, it is difficult to monitor dynamic processes and transmembrane charge transport.

Liberman and Topaly (1969) observed that the conductivity of a lipid bilayer to lipophilic cations could be considerably increased by the presence of small amounts of hydrophobic anions. They explained such a phenomenon simply as the increased binding constant of the cation in the anion-loaded bilayer. More recent studies (Drain et al., 1989; Drain and Mauzerall, 1992; Mauzerall and Drain, 1992) have shown that the conductivity of lipophilic ions across lipid bilayers can be dramatically controlled or gated by formation of oppositely charged ions inside the bilayer. The photoformation of the cation of magnesium octaethylporphyrin (MgOEP) in the bilayer can increase the transmembrane ionic current carried by tetraphenylborate ($TPhB^-$) anions ~10fold. We have now found that the photoinduced increase of the membrane conductance can reach ~100-fold by chloro substitution on the phenyls of $TPhB^-$. The translocation rate of P^+ across the bilayer is similarly increased ~100-fold by the presence of borate anions. This ion-gating effect offers a new tool for probing ion interactions within the bilayer and the mechanisms of charge transport across the lipid bilayer. It also offers the possibility of making efficient transmembrane charge transfer systems.

Received for publication 31 October 1995 and in final form 3 April 1996.
Address reprint requests to Dr. David Mauzerall, The Rockefeller University, 1230 York Avenue, New York, NY 10021. Tel.: 212-327-8218; Fax: 212-327-8853; E-mail: mauzera@rockvax.rockefeller.edu.

0006-3495/96/07/295/14 $2.00

MATERIALS AND METHODS

1,2-Diphytanoyl-3-sn-phosphatidylcholine (DPPC) and L-α-lecithin were from Avanti Polar Lipids (Alabaster, AL). Magnesium octaethylporphyrin (MgOEP), chlorophyll *a* (Chl *a*), and sodium tetrakis(*p*-fluorophenyl)bo-

rate (p-TFPhB$^-$) were from Aldrich Chemical Co. (Milwaukee, WI). Potassium tetrakis(*p*-chlorophenyl)borate (p-TCPhB$^-$) was from Fluka Chemika (Buchs, Switzerland). Cholesterol, phloretin, and sodium tetraphenylborate (TPhB$^-$) were from Sigma Chemical Co. (St. Louis, MO). Sodium tetrakis(*m*-chlorophenyl)borate (m-TCPhB$^-$) and sodium tetrakis(*m*-fluorophenyl)borate (m-TFPhB$^-$) were synthesized by a reported method (Jarzembowski et al., 1974). Magnesium etioporphyrin I (MgETP) and ethyl chlorophyllide were prepared from etioporphyrin I dihydrobromide and *Ailanthus altissima*, respectively, according to the reported procedures (Chow et al., 1975; Fuhrhop, 1981).

The lipid membrane was formed in a 1.5-mm-diameter hole in a 0.38-mm-thick Teflon sheet symmetrically dividing a 4-ml polyethylene cell with glass windows, bathed in symmetrical 0.1 M NaCl solutions containing 10 mM HEPES buffer (pH 7.8). The lipid solution consisted of 18 mM DPPC or 50 mM lecithin and 3.6 mM magnesium porphyrin or chlorophyll in *n*-decane. The capacitance of the membrane was determined from the square-wave current response to the applied triangle-wave voltage across the membrane in the 0.5–50-kHz range below ±20 mV. The capacitance and resistance of the membrane were, respectively, ~5 nF and $\sim 10^{10}$ Ω, if no lipophilic ions were present in the systems. They were, respectively, about ~50 nF and $\sim 10^8$ Ω on the >0.1-s time scale if 4 μM borate anions were in the bathing solutions. The borate was always added symmetrically to the bathing solutions on both sides after the lipid membrane was formed. To keep the systems stable for a long time and yet give the largest signal, 4 μM borate concentration was used in most experiments. The dark conductance of the membrane shows that the partition of borate anions in the lipid bilayer is saturated by space charge at this concentration (Mauzerall and Drain, 1992). Stock solutions of the borates were made using ethanol as the solvent. The ethanol content in the bathing solutions was kept below 0.5%.

The standard symmetric system for measuring the photogating effect was 0.3 mM sodium anthraquinone-2-sulfonate (AQS) symmetrically added to the bathing solutions as electron acceptor, the saturating concentration for the photovoltage (Ilani and Mauzerall, 1981), and 40 mV voltage applied across the membrane through two calomel electrodes to drive the ionic current. Activation energies of the gating borate transport were determined by repeating the measurement at temperatures between 6 to 30°C in a water-jacketed cell. The standard asymmetric system for observing the photodriven transmembrane charge transport was, after lipid membrane formation, 0.3 to 0.5 mM AQS added to one side of the membrane as electron acceptor and 4 mM ferrocyanide added to the side opposite to the acceptor as electron donor. For some measurements, the electron donor was absent in the systems or present on the same side with the acceptor, which has been noted in the text. There was no outside applied voltage for the asymmetric systems, except for a measurement of the current in Fig. 4.

The current and voltage across the membrane were measured through two calomel electrodes with saturated KCl bridges (Fisher Scientific, NJ) immersed in the bathing solutions on each side of the membrane. The potential difference and the resistance between the two electrodes themselves were below 0.6 mV and 2 kΩ, respectively. The current was monitored by a fast operational amplifier (model 1021; Teledyne, Philbrick, MA) with a homemade feedback circuit of adjustable gain and time constant. Typically, the operational amplifier was set at 10^6 to 10^8 V/A with a time constant of 10 μs to 1 ms to measure currents. For the photogating current measurement, a voltage was applied between the two electrodes, using a variable series voltage source. The sign of the applied voltage was that on the side opposite the acceptor for the asymmetric system. The photovoltage was monitored with a Stanford Research Instruments SR560 low-noise preamplifier (10^8 Ω input impedance, 1 MHz frequency response). The confirming measurements for photovoltage were carried out using a Keithley 617 programmable electrometer with 10^{14} Ω input impedance, because the input impedance of an SR560 preamplifier is not high enough compared to the resistance of the membranes under some conditions. The triangle-wave voltage for measurements of membrane capacitance was from an Exact model 190T function generator. The light pulse at 590 nm with 1 μs full width at half-maximum was from a Candela SLL-250 flash-lamp pumped dye laser, using rhodamine 6G in methanol. The pulsed light with signal-saturated intensity (~1 mJ) was always used to illuminate the membrane unless otherwise noted. A 300-W tungsten/halogen projector was used to illuminate the membrane for the continuous light experiments. It resulted in ~130 mW cm^{-2} light in the ~400–600 nm range at the membrane after filtering by 2 cm, 0.2 M $CuSO_4$ aqueous solution. Other details about the entire apparatus can be found elsewhere (Mauzerall and Drain, 1992).

RESULTS

The membrane systems and the probing methods are schematically shown in Fig. 1. The symmetric membrane system for observing the photogating effect (Fig. 1 *A*) can be concisely depicted as acceptor/sensitizer/acceptor plus applied voltage, and the asymmetric system for the photodriven transmembrane charge transfer (Fig. 1 *B*) as acceptor/sensitizer/donor. Here the / stands for the membrane-solution interface. In all of the aqueous solutions, sufficient passive ions (0.1 M NaCl) were present, so the other ions carry an insignificant portion of the current.

Photogating currents driven by applied voltage

Sensitivity to component structure

Fig. 2 *A* shows the photogenerated increase of the voltage-driven current carried by borate anions after a 1-μs pulsed illumination to the symmetrical acceptor/sensitizer/acceptor system, and the striking increases with small structural changes in the borates. The increase in the current is the photogating effect named earlier (Drain et al., 1989; Mauzerall and Drain, 1992). It arises from the photoformation of P^+ by electron transfer from the excited porphyrin in the bilayer to the ionic acceptor across the membrane-solution interface. Current traces symmetric about the zero level in Fig. 2 are obtained when the sign of the applied voltage is reversed. In the dark, the voltage-driven current across the DPPC bilayer of all borate anions at saturating concentrations is 0.1–0.2 nA at 40 mV. The currents on the >0.5-ms time scale after illumination increase linearly with the applied voltage in the ±80 mV range (data not shown), i.e., they obey Ohm's law. Because the time constants do not change appreciably, the integral of $I\ dt$ over the 0.5–3000-ms time range is not constant with increased voltage (data not shown). Thus these are enhanced voltage-driven ionic currents across the bilayer, not charge displacement currents. They differ from the fast currents in uni-charged membranes, where the time constant decreased as the current increased with voltage, thus conserving charge (Andersen et al., 1978). The maximum enhanced current of p-TCPhB$^-$ (Fig. 2 *A*, *curve a*) is ~100 times its dark current. The photogating effect of this system is over 10 times greater than that of TPhB$^-$ (Fig. 2 *A*, *curve e*) and is caused only by substituting chlorine for hydrogen at the *para* position of the phenyls. The enhanced current decreases when chloro substitution is replaced by fluoro or occurs at the *meta* position of the phenyl groups (Fig. 2 *A*, *trace a* versus *b*, *c*, and *d*). Note that the current transients

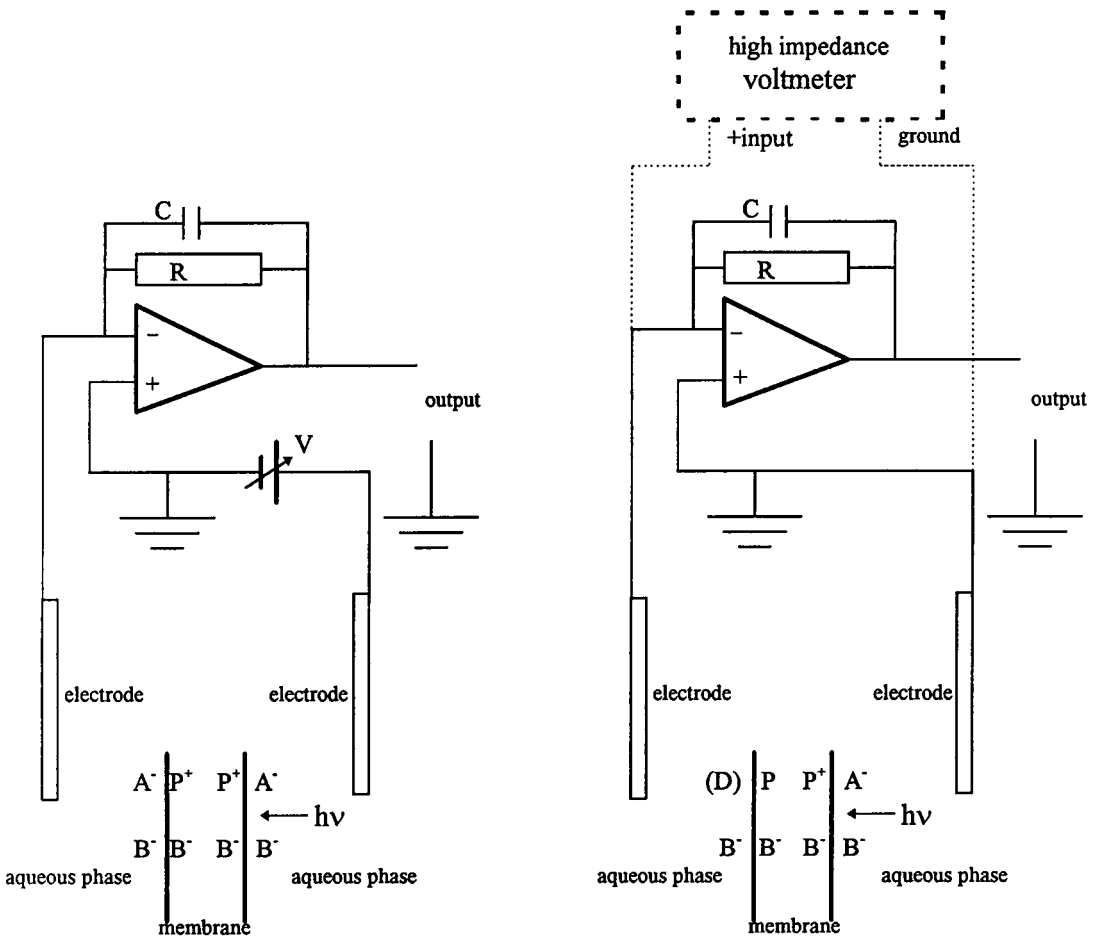

FIGURE 1 Schematic diagrams of membrane systems and probing methods. B^- represents hydrophobic borate anions. P and P^+, respectively, represent neutral and positively charged porphyrins. A^- represents the reduced electron acceptor. Other details have been interpreted in Materials and Methods. The symmetric membrane system (A, acceptor on both sides) with applied voltage is used for measuring the photogating current. The asymmetric membrane system (B, acceptor on right side only) without applied voltage is used for monitoring the photodriven charge transfer by measuring both currents and voltages. D represents the electron donor, which is added to the side opposite that of the acceptor when the transmembrane movement of P^+ is monitored. Dotted lines represent the circuit for voltage measurements.

appearing on the <1-ms time scale are opposite in sign from that expected for the applied voltage (Fig. 2). These transients arise from ion displacements or depolarizations internal to the membrane.

The sensitivity of the photogating current of p-$TCPhB^-$ to the structure of P^+ is shown in Fig. 2 *B*. The minor replacement of four ethyls by methyls on the porphin ring from MgOEP to MgETP (Fig. 2 *B*, *curve a* versus *f*) decreases the photogating effect by about one-half. The more polar chl *a* produces only a small (threefold; Fig. 2 *B*, *curve g*) photogating effect. These decreases are not caused by less absorption of light, because the light pulse is saturating and the separately measured photovoltages are similar for all these pigments.

The photogating effect is also strongly affected by the specific bilayer-forming lipids (Fig. 2 *C*). The bilayer formed from lecithin (Fig. 2 *C*, *curve h*) shows an impressive fivefold greater photogating current than that from DPPC (Fig. 2 *C*, *curve a*), but also has an eightfold greater dark current. Lecithin is more mobile and flexible than DPPC in a bilayer (Redwood et al., 1971). The addition of 10% phloretin to the lecithin bilayer decreases the dark current by 80% and the photogating current by 40% (Fig. 2 *C*, *curve j* versus *h*), but the addition of 5% cholesterol increases the dark current by fivefold, yet has a small effect on the photogating current (~10% decrease; Fig. 2 *C*, *curve i* versus *h*). The presence of phloretin and cholesterol may, respectively, decrease and increase the positive internal potential of the bilayer (Andersen et al., 1976; Franklin and Cafiso, 1993), so their influence on the dark current conductivity is as expected from the electrostatic effects. But their smaller effects on the photogating current cannot be

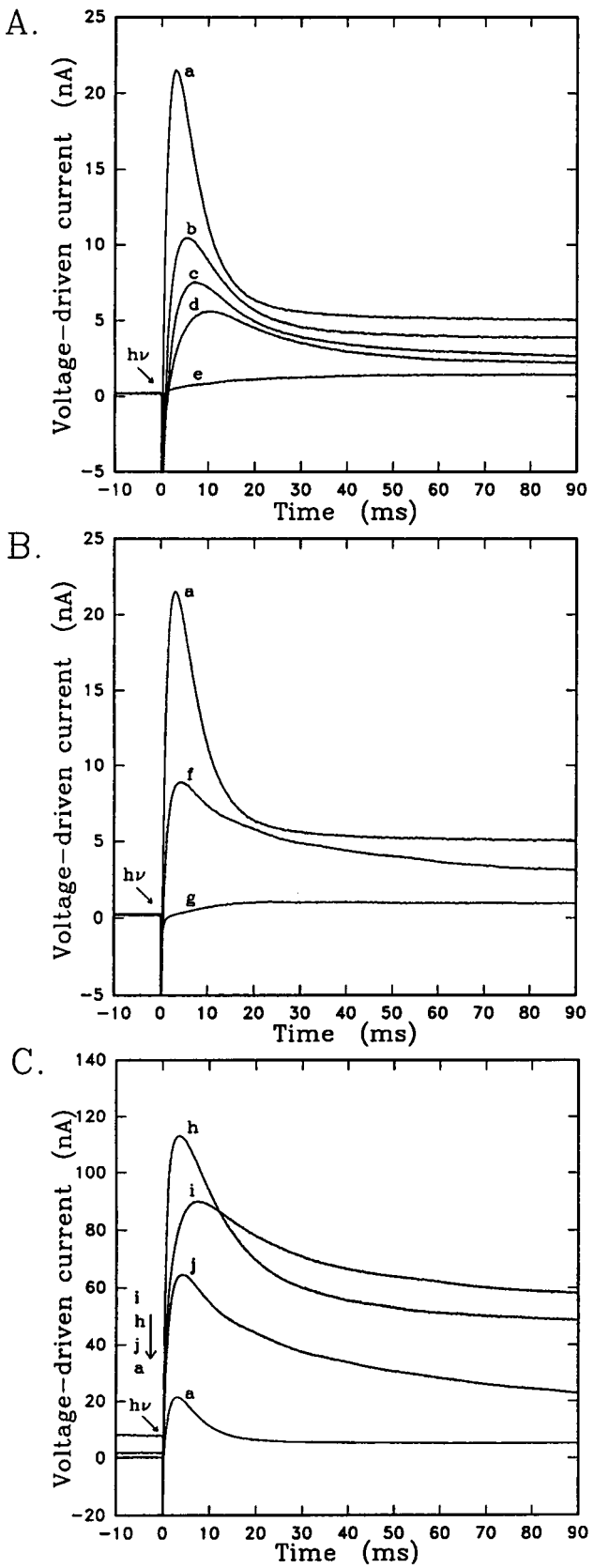

similarly explained. The presence of phloretin and cholesterol in the absence of borates decreases the capacitance of the membrane by ~50% and ~20%, respectively. The dielectric weighted thickness of the bilayers is increased by these polar molecules, so their function in the bilayer is complicated.

The above results demonstrate that the photogating effect is very sensitive to the structures of both hydrophobic anions and photoformed cations as well as lipids. The concentrations of the photoformed P^+ cation are the same in the presence of different borates, as proven by the same maximum photovoltage (Fig. 2; Sun and Mauzerall, 1996). The 10-fold further enhancement of the translocation rate of p-TCPhB$^-$ anions over that of TPhB$^-$ anions cannot be explained by the positive potential caused by porphyrin cations, because the electrostatic energy is the same, to first order, for the different-sized anions. Thus, the photogating effect is not totally caused by electrostatic effects. These results suggest that cation-anion aggregates are involved in the enhancement of conductivity.

Fig. 3, *A* and *B*, shows the dark and photoconductivities of the MgOEP-DPPC bilayer at different p-TCPhB$^-$ and p-TFPhB$^-$ concentrations, respectively. The dark conductivity increases linearly with the concentration of borate anions in the <0.2 μM range and becomes saturated at higher concentrations because of space charge. The data can be fit very well (Fig. 2, *filled circles and solid curve*) using the published space charge model (Mauzerall and Drain, 1992) and the parameters similar to those of TPhB$^-$. The binding constants for the substituted borates are within a factor of 2 of those of the unsubsituted borate (Benz, 1988). Our fit to the dark conductance (Fig. 3) supports this value of binding constant. For the substituted borates, however, 10–30-fold photogenerated enhancement of the conductivity is observed at low concentration (10^{-8} M), where little space charge is present in the bilayer and the enhancement by TPhB$^-$ is negligible (figure 2 in Mauzerall and Drain, 1992). The photoinduced conductivity of the substituted borate anions also saturates with increasing concentration. This indicates that the borate concentration in the bilayer is limiting. The large photogating effect at low concentrations indicates that the effect does not arise only from space

FIGURE 2 The photogating currents caused by a 40-mV applied voltage and a 1-μs pulsed illumination are plotted versus time. Magnesium porphyrin (3.6 mM) was in the bilayer-forming solution. AQS (0.3 mM) is present on both sides of the bilayer as an electron acceptor. Borate (4 μM) is symmetrically added to the bathing solutions after the bilayer is formed. The energy of the light pulse at 590 nm is ~1 mJ at the membrane. The time constant of the circuit is 0.01 ms, except for the systems containing TPhB$^-$ or Chl *a* (0.1 ms). (*A*) Currents for different borate anions: curve a, p-TCPhB$^-$; curve b, p-TFPhB$^-$; curve c, m-TCPhB$^-$; curve d, m-TFPhB$^-$; curve e, TPhB$^-$. (*B*) Changes of the p-TCPhB$^-$ current with the structure of photosensitizer in the DPPC bilayer: curve a, MgOEP; curve f, MgETP; curve g, Chl *a*. (*C*) Changes of the p-TCPhB$^-$ current across the MgOEP bilayer with composition of the lipid solution: curve a, DPPC; curve h, L-α-lecithin; curve i, lecithin with 5% cholesterol (mol/mol); curve j, lecithin with 10% phloretin (mol/mol).

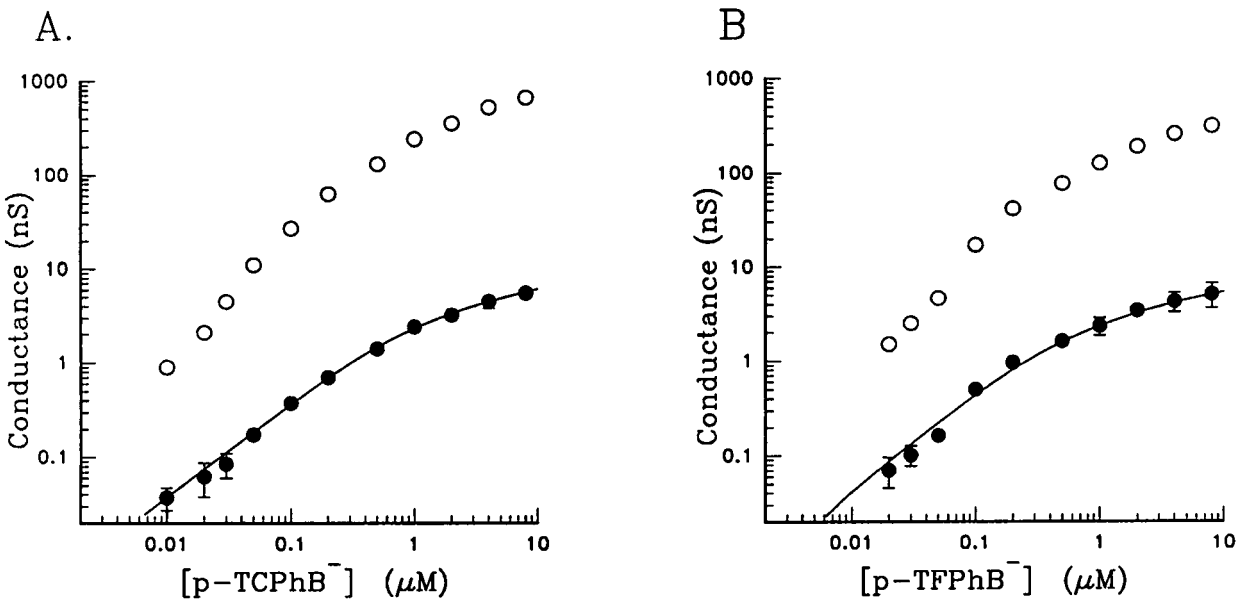

FIGURE 3 The dark and photoconductivities of the MgOEP-DPPC bilayer with borate anions are plotted versus their concentrations. The dark conductivity is the measured steady current on the time scale of seconds divided by the 40-mV applied voltage. The photoconductivity is the maximum in the enhanced voltage-driven current at ~5 ms minus the dark current divided by 40 mV. Open circles represent the maximum photoconductivities. Filled circles represent the dark conductivities. Solid curves represent the fit of the space charge model (Mauzerall and Drain, 1992) to the dark conductance of borate anions with parameters $d_m = 8$ nm, $A_m = 8 \times 10^{11}$ nm^2, $\beta = 2 \times 10^5$ nm, $\mu \cong 15$ nm^2 s^{-1} V^{-1}. (*A* and *B*) p-TCPhB$^-$ and p-TFPhB$^-$ systems, respectively. The experimental conditions are the same as those in Fig. 2.

charge. Other interactions of the ions must contribute to the nonlinear enhanced conductivity.

The large enhanced photogating effect can also be observed under steady-state conditions. Continuous illumination of the MgOEP-DPPC bilayer causes a 50–60-fold increase of the voltage-driven current in the presence of 4 μM p-TCPhB$^-$. This enhanced current is basically stable on the minute time scale.

Temperature dependence

The temperature dependence of voltage-driven dark and photogating currents was determined. The dark currents and photogating currents and their half-rise times with 40 mV of applied voltage at different temperatures for p-TCPhB$^-$, p-TFPhB$^-$, and TPhB$^-$ are listed in Table 1. The dark conductivities are basically the same at a given temperature for all of the borates, but the photoconductivities vary by over an order of magnitude. The translocation rates of borate anions in both dark and light have positive activation energies (shown in Table 1), and the E_a values of the photogating current are two to three times those in the dark for all of the borates. Their average values are, respectively, 13 and 5 kcal mol^{-1}. The activation energy for the current rise time is intermediate, 10 kcal mol^{-1}. The differences in E_a between different borates are very small (<2 kcal mol^{-1}). Both the E_a values in the dark and their insensitivity to the structural changes of borates are similar to results reported by Benz on the activation energy of translocation rates using the charge pulse method (Benz, 1988). These results indicate that any changes in the Born energy caused by different effective ion radii of borates has little effect on the activation energy. If the photoformation of porphyrin cations only canceled the space charge and added positive potential to the bilayer, one would not expect the E_a of borate movements to increase compared to that in the dark, because the central energy barrier for the ion transport under the photo condition would be smaller. The ~2-fold larger E_a of the enhanced ion translocation affords further support for the hypothesis that the enhancement arises in an ion aggregate (see Discussion).

Enhanced decay of photogating currents and of P$^+$ by a *trans* donor

The photogating effect can be caused even if P$^+$ cations are photoformed at a single membrane interface of the asymmetric system, which has an electron acceptor only in one bathing solution. By adding an electron donor to the side opposite the acceptor, the transmembrane movements of P$^+$ can be studied by the photogating effect. The presence of a *trans* donor increases the decay rates of photogating currents and of P$^+$.

When 40 mV is applied across the MgOEP-DPPC bilayer in the presence of 4 μM p-TCPhB$^-$ in the dark, a 0.2-nA offset steady current is observed. If the acceptor AQS is present only on the ground side of Fig. 1 *A*, pulsed illumination causes a 20–30-fold increase in the offset current on the >15-ms time scale (Fig. 4, *curves a* and *d*). The increased offset current caused by the photoformation of the

TABLE 1 Temperature dependence of dark current (I_d), photogating current (I_p), and its half-rise time ($t_{1/2}$) as well as the activation energy (E_a) of each process (40 mV applied voltage, 4 μM borates)

T (°C)	I_d (nA)	I_n (nA)	$t_{1/2}$ (ms)
p-TCPhB$^-$			
6	0.13	2.4	1.7
10	0.17	4.7	1.2
15	0.21	8.2	0.92
20	0.24	12	0.70
25	0.28	15	0.57
30	0.31	19	0.48
E_a (kcal mol^{-1})	5.5	13	9.3
p-TFPhB$^-$			
6	0.14	1.3	8.2
10	0.19	2.5	6.0
15	0.23	4.3	4.0
20	0.26	5.8	2.8
25	0.28	7.0	2.3
30	0.31	9.5	2.0
E_a (kcal mol^{-1})	5.5	13	10
TPhB$^-$			
6	0.11	0.21	30
10	0.14	0.37	22
15	0.17	0.60	14
20	0.19	1.1	10
25	0.21	1.3	8.0
30	0.24	1.5	6.1
E_a (kcal mol^{-1})	4.8	14	11

P^+ cations is the photogating current studied in the symmetric system with electron acceptors on both sides (Drain et al., 1989; Drain and Mauzerall, 1992; Mauzerall and Drain, 1992). When a saturating concentration of electron donor is added, the changes of the photogating current are shown by curves a versus b and d versus c in Fig. 4, respectively, for the opposite signs of applied voltage. The enhanced offset current on the 100-ms time scale is lost, even if the donor is present on the side opposite the acceptor.

The decay rate of the slow photogating current represents the lifetime of the P^+ cation, because the photogating effect is proportional to the amount of P^+ in the membrane (Drain and Mauzerall, 1992). The decay time of the photogating current is ~5 s for the system with any one of the borates in the absence of an electron donor. Thus the lifetime of P^+ in the membrane is quite long in the presence of borate anions. This is direct proof that borate anions do not reduce P^+ cations and the enhanced conductivity of borate anions arises from the presence of the photoformed P^+ cations. Fig. 5 shows the decay rate constants of the photogating current at different low concentrations of ferrocyanide when present on the acceptor side or on the opposite side. An apparent second-order rate constant of the electron transfer from ferrocyanide to P^+ can be obtained from the slopes on the linear scales. It is 2.2×10^7 M^{-1} s^{-1} when ferrocyanide is on the same side of the bilayer as the acceptor, which is slightly smaller than that (3.5×10^7 M^{-1} s^{-1}) of the egg

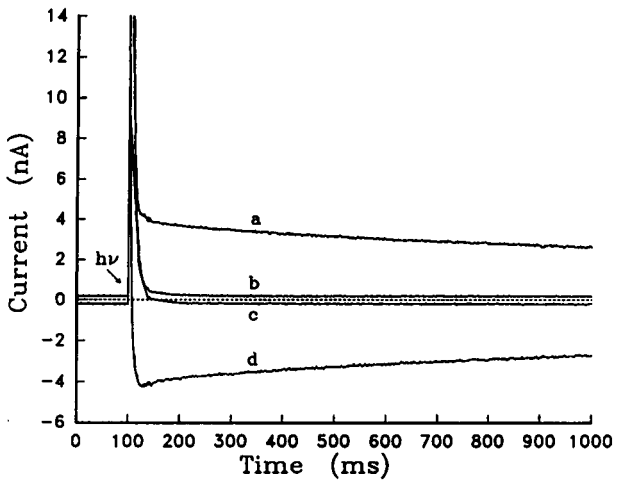

FIGURE 4 The currents caused by applied voltage across the asymmetric MgOEP-DPPC bilayer and 1-μs pulsed illumination of the membrane are plotted versus time. The voltage sign refers to that on the electrode on the side opposite the acceptor. The other electrode is grounded. p-TCPhB$^-$ (4 μM) is symmetrically present. +40 mV (*curve a*) and −40 mV (*curve d*) are applied without a donor. +40 mV (*curve b*) and −40 mV (*curve c*) are applied, and 50 μM ferrocyanide is present on the side opposite the acceptor.

lecithin membrane system in the absence of borates (Hong and Mauzerall, 1976). The apparent rate constant is 100-fold less, 2.4×10^5 M^{-1} s^{-1}, when ferrocyanide is on the side opposite the acceptor. The difference of the apparent second-order rate constants indicates that the transmembrane charge transfer is limited by the translocation of P^+, even if borate anions are present in the membrane. The translocation rate constant of the photoformed P^+ across the

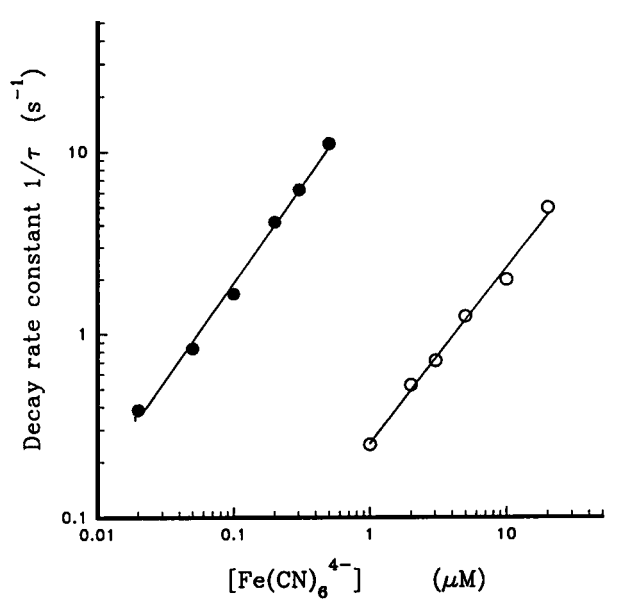

FIGURE 5 The decay rate constants of the slow photogating current with donor on the same side (●) and on the side opposite (○) the acceptor are plotted versus concentration of the donor, ferrocyanide, on log-log scales. The slope of the lines is unity.

membrane could be obtained from the saturation of the transmembrane P^+ decay rate at high concentrations of ferrocyanide. Unfortunately, the decay times of the photogating currents shorter than 50 ms cannot be determined when the concentration of ferrocyanide on the side opposite the acceptor is higher than 20 μM, because the photodriven currents (to be discussed in the following section) across both the membrane and interfaces are much larger on the <50-ms time scale than the photogating current driven by applied voltage (Fig. 4). The rapid decay of the photogating current caused by the *trans* donor (Fig. 4) proves that the presence of borate anions largely increases the transmembrane translocation of P^+, because the bilayer crossing time of free P^+ is longer than 0.1 s (Woodle and Mauzerall, 1986) and the presence of a *trans* donor does not cause extra currents on the <0.1-s time scale in the absence of borates. This is consistent with the P^+ translocation time of ~10 ms inferred from the internal charge movement discussed in the next section (Figs. 7 *A* and 8).

Photodriven charge movements under asymmetric conditions

Steady-state photodriven current

For the 0.5 mM AQS/3.6 mM MgOEP/4 mM ferrocyanide system, Fig. 6 shows a ~100-fold increase of the transmembrane photodriven current (590 versus 5 pA) caused by the symmetric addition of 4 μM p-$TCPhB^-$ anions to the bathing solutions and continuous illumination. The increase in photodriven current by the presence of borate anions indicates that the photodriven P^+-mediated redox flux from AQS to ferrocyanide and thus the translocation rate of P^+ across the bilayer have also been enhanced ~100-fold. A negative current (−160 pA) is observed in the absence of an electron donor. This arises from the electrostatic ion pumping effect (Sun and Mauzerall, 1996). The presence of 4 μM p-$TFPhB^-$ in the system instead of p-$TCPhB^-$ also causes a ~100-fold increase in the photodriven current, whereas 4 μM $TPhB^-$ produces only a 30–40-fold increase in the steady-state current. Similar photodriven currents (580 and 5 pA, respectively, in the presence and absence of p-$TCPhB^-$) are observed for the system with 3.6 mM MgETP in the bilayer instead of MgOEP. A very small transmembrane current (<1 pA) is observed with the Chl *a*-containing bilayer in the absence of borate anions. Thus the chlorophyll cation has an even lower mobility than the cation of MgOEP in the lipid bilayer. The current is increased only to 25 pA by the addition of 4 μM p-$TCPhB^-$ to the bathing solutions. A lipid bilayer containing 3.6 mM ethyl chlorophyllide shows behavior similar to that containing Chl *a* in the absence (<1 pA) and presence (30 pA) of borates on continuous illumination. This indicates that the slow translocation rate of chlorophyll cations is mainly caused by the polar chlorin headgroup and not by the long phytyl chain.

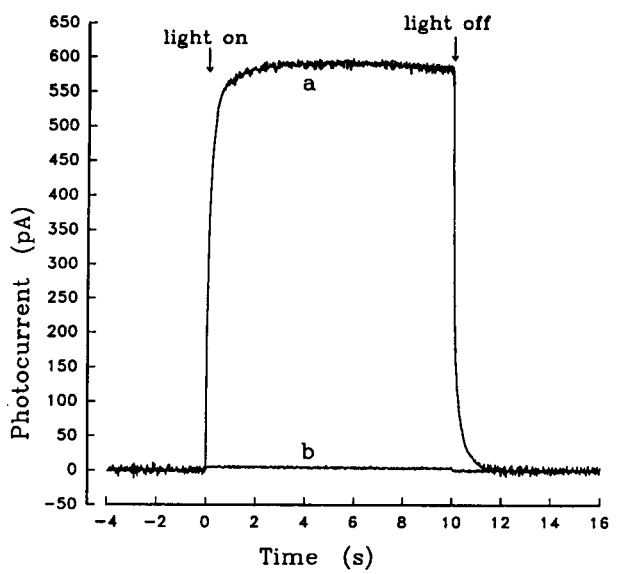

FIGURE 6 The steady-state photodriven currents caused by 130 mW cm^{-2} of white continuous illumination of the asymmetric lipid membrane are plotted versus time. MgOEP (3.6 mM) is present in the DPPC bilayer, and saturating concentrations of acceptor (0.5 mM AQS) and donor (4 mM ferrocyanide) are present on opposite sides. curve a, 4 μM p-$TCPhB^-$ is added to both sides. curve b, No borates are present in the system. The presence of p-$TCPhB^-$ increases the low-frequency (40–60-Hz) noise by ~10 times under both dark and photo conditions (*curve a*) because of a 10-fold increase in the membrane capacitance.

Pulsed photodriven current

The results with pulsed light illumination of the asymmetric membrane (i.e., separating acceptor and donor) afford kinetic evidence that the transport of photoformed P^+ cations across the lipid bilayer is also drastically increased by the presence of the borates. The sensitivity of the P^+ transit time to the structure of borates is direct evidence that porphyrin cation–borate anion aggregates are involved in the conductance changes. When the AQS/MgOEP/no donor system with p-$TCPhB^-$ or p-$TFPhB^-$ is illuminated by a 1 μs pulse of light, a shoulder or peak in the current is observed on the 0.5–15-ms time scale after the positive current transient on the <0.5-ms time scale (Fig. 7, *A* or *B*, *curve b*). The latter is caused by photodriven electron flow from the excited MgOEP to the aqueous acceptor and is broadened by the displacements of borate anions. The addition of 50 μM ferrocyanide on the side opposite the AQS causes a large increase in the current in the 0.5–20-ms range for the 4 μM p-$TCPhB^-$ and the p-$TFPhB^-$ systems (Fig. 7, *A* and *B*, *curve a* versus *b*). The extra current arising from charge transfer to ferrocyanide is shown by curve c in Fig. 7, *A* and *B*. The half-rise time and half-decay time of the extra current are, respectively, 1–2 ms and 10–20 ms for both the p-$TCPhB^-$ and p-$TFPhB^-$ systems. The total extra charge moved in 0.5–40 ms is ~200 pC, which is about twice the total charge moved by the donor free systems (~130 and ~100 pC for the p-$TCPhB^-$ and p-$TFPhB^-$

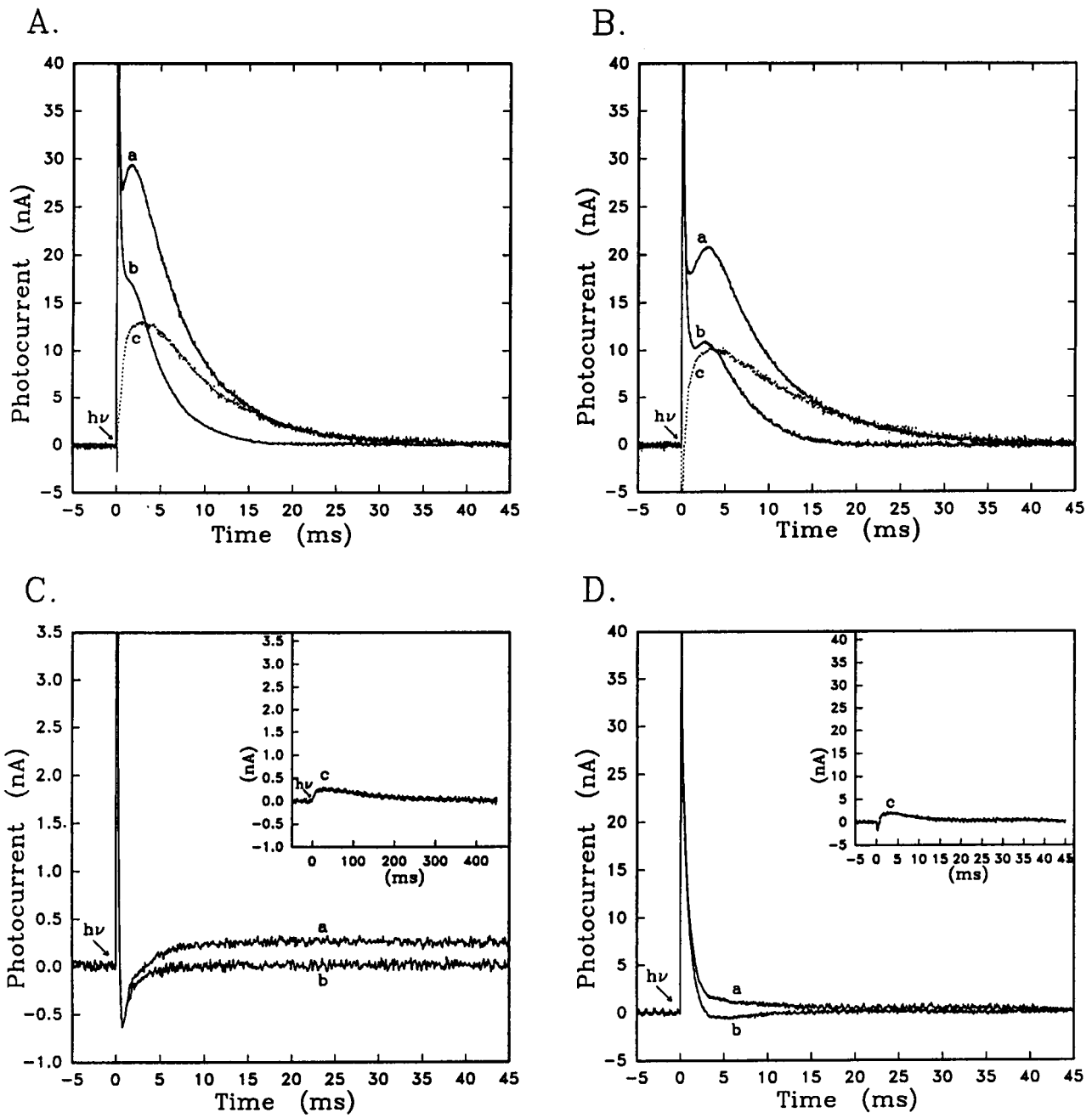

FIGURE 7 The photodriven currents caused by a 1-μs saturating pulsed illumination of the asymmetric membrane are plotted versus time. The time constant of the current amplifier is 0.01 ms. AQS (0.3 mM) is added to one side of the DPPC bilayer containing 3.6 mM MgOEP. Borate (4 μM) is symmetrically present in the systems. curve a, 50 μM ferrocyanide is added on the side opposite the AQS. curve b, No electron donor is added in the system. curve c, The extra photocurrent caused by the addition of the electron donor, i.e., the difference of curves a and b. (*A*, *B*, and *C*) Systems with a MgOEP-DPPC bilayer and containing, respectively, p-TCPhB$^-$, p-TFPhB$^-$, and TPhB$^-$. (*D*) p-TCPhB$^-$ system with a Chl *a*-DPPC bilayer.

systems, respectively). The extra photocurrent is caused by electron transfer from the donor to the transported P^+ cation near the donor interface. Thus the photoformed P^+ cations cross the hydrocarbon region of the membrane on the 1–10-ms time scale, but only in the presence of the borate anions.

The system without borate anions and with or without donor only shows the *C* d*V*/d*t* displacement current similar to curve b in Fig. 7 *C* after pulsed illumination of the membrane. In the presence of 4 μM TPhB$^-$, the addition of donor causes only a weak positive current (Fig. 7 *C*, *curve a* versus *b*). Both the half-rise time (~10 ms) and half-decay time (~200 ms) of the extra current (Fig. 7 *C*, *curve c*) are ~10-fold longer than those of the p-TCPhB$^-$ and p-TFPhB$^-$ systems. The total extra charge moved by the TPhB$^-$ system is only ~40 pC, and it takes ~200 ms to cross the

membrane. The concentrations of the borate anions in the bilayer are roughly equal, because their partition constants are almost equal (Benz, 1988). The above results show that the enhanced transmembrane P^+ transport depends sensitively on the structure of the borate anion, not only on its negative charge, for the photodriven system, as for the voltage driven system (see Photogating Effect, above). This enhanced effect is similarly affected by the structure of the P^+ cation. For the Chl *a* system with p-TCPhB$^-$, the addition of ferrocyanide on the side opposite the acceptor causes only one-tenth the photocurrent (Fig. 7 *D*, *curve a* versus *b*) as that for the MgOEP system (Fig. 7 *A*, *curve a* versus *b*) on pulsed illumination. The extra charges moved on the >0.5-ms time scale are ~10–20 pC (Fig. 7 *D*, *curve c*), which is only 5–10% of that in the MgOEP bilayer. Membranes containing ethyl chlorophyllide give almost the same photocurrent traces as those with Chl *a* (Fig. 7 *D*) on pulsed illumination, showing again that the polar headgroups and not the phytyl chain are responsible for the lesser activity.

Pulsed photovoltage

The time-resolved measurements of photovoltages can afford direct proof of charge separation across the interface or the bilayer and of their respective time scales.

The presence or absence of a donor on the side of the bilayer opposite the acceptor has no effect on the maximum of the positive photovoltage or on its slow decay on the <0.1-s time scale in the absence of borates (Fig. 8, *curves c* and *d*). However, the presence of donor on the side opposite the acceptor and the symmetric addition of substituted borate anions in the system cause a dramatic resurgence of a positive voltage after pulsed illumination (Fig. 8, *curve a*). Unsubstituted TPhB$^-$ has a slower and much smaller effect (Fig. 8, *curve b*). The symmetric addition of 4 μM p-TCPhB$^-$ to the system shifts the starting time of the resurgence of photovoltage from ~100 ms (Fig. 8, *curve c*) to ~1 ms (Fig. 8, *curve a*). The delayed photovoltage decays with the RC time (~5 s) of the measuring circuit. The capacitance of the membrane increases ~10-fold (from 5 to 50 nF) in the 0.5-ms time domain in the presence of p-TCPhB$^-$. The increase of capacitance on the millisecond time scale explains why the observed half-rise time (~20 ms) of the resurgent voltage (Fig. 8, *curve a*) is longer than that (<10 ms) expected from the pulsed photocurrent in the 1–10 ms range (Fig. 7 *A*, *curve c*). The P^+ cation crosses the membrane with a bulk transit time of 10 ms in the presence of p-TCPhB$^-$ and is neutralized by the electron donor at the interface opposite the acceptor, thus transferring positive charge completely across the membrane. The complete separation of the photoformed negative and positive charges by the membrane causes an increase in the voltage. The ~4 mV delayed photovoltage indicates that ~200 pC charge has been completely separated by the membrane (calculated on 50 nF, the measured capacitance in this time range). This is consistent with the moved charge calculated from the extra current caused by the presence of donor (Fig. 7 *A*, *curve c*). In the absence of donor and in the presence of borates, a delayed negative voltage is observed, which is attributed to electrostatic ion pumping (Sun and Mauzerall, 1996).

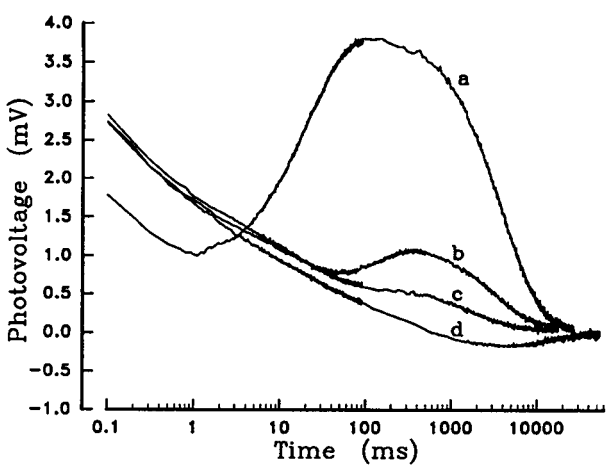

FIGURE 8 The photovoltages caused by 1-μs pulsed illumination of the asymmetric MgOEP-DPPC bilayer are plotted versus log time. The electrode on the side opposite the acceptor is connected to the positive input of the voltmeter. curve a, 4 μM p-TCPhB$^-$ is added symmetrically in the presence of 50 μM ferrocyanide (donor) on the side opposite the acceptor. curve b, 4 μM TPhB$^-$ replaces p-TCPhB$^-$. curve c, Only donor is present without borates. curve d, Neither electron donor nor borates are present.

DISCUSSION

The enhanced conductivity of lipid bilayers in the presence of hydrophobic ions of opposite charge cannot be explained simply as increased binding (Liberman and Topaly, 1969), because we have directly observed the ~10-fold decrease of transmembrane transit time of ions (Fig. 7 *A*, *curve c*, versus that in Fig. 7 *C* and Fig. 8, *curves a* versus *b*). The enhancement is most likely explained by the formation of ion aggregates. The interfacial exchange of the mobile hydrophobic ion and the shuffling of ion pairs in the aggregate explains the increased mobility of both ions. A specific mechanism for the enhanced transmembrane transport of P^+ cations is the dynamic ion chain mechanism (Drain and Mauzerall, 1992). In this model, chains of alternatively charged ions across the bilayer are formed by transient binding between photoformed P^+ cations and borate anions. The interaction between P^+ and borate anions in the ion chain is dynamic. This ion chain mechanism is similar to the mechanism for the conductance of anions or cations through ion channels in that these ions are thought to hop along the polar sites of the channel. The Born and image energies of the ion chain are significantly less than those of the individual ion. The Born electrostatic energy of a contact ion pair of equal-sized ions is one-half that of the individual ions, and the image energies will further reduce the total energy. Both the P^+ cation and the borate anion can hop

along the ion chain, via rotations of neutral ion pairs, to cross the membrane. The arguments in favor of this hypothesis can be summarized as follows:

1. Insufficient concentrations of porphyrin cations are formed to completely cancel the borate space charge required to explain the photogating effect on purely electrostatic grounds (Drain and Mauzerall, 1992). The enhancement of the conductivity of the substituted borate anions at low concentrations, where space charge is negligible, also indicates a different mechanism of the enhanced ion translocation.

2. The enhanced conductivity is extremely sensitive to structural changes in the hydrophobic ions of either sign (Fig. 2), whereas the dark conductivities are almost the same for all of the borates (Table 1). A decrease in Born energy by an increase in the effective radii in the substituted borates should increase the dark conductivity, but the Born energy should not be changed by the presence of the photoformed P^+ if the borate anion moves alone. Although the electrostatic potential energy of borate anions in the bilayer is certainly lowered by the positive potential of porphyrin cations, the effect on all of the borate anions should be comparable, because the densities of positive and negative charges are roughly the same. Thus, the minor decrease in Born energy and the positive potential of porphyrin cations cannot explain the ~10-fold larger ratio of the photo to dark conductivities for p-$TCPhB^-$ anion. This can be easily explained as specific interactions in the close molecular aggregates. Structure-specific interactions of tetraphenyl borates and large cations have been observed (Yang et al., 1992; Armitage et al., 1993).

3. The ~2-fold larger activation energy of the enhanced ion transport (Table 1) is not expected from electrostatic effects. However, the alignment and rotation of porphyrin cation-borate anion ion pairs require extra activation energy for conduction in an aggregate. The Born electrostatic energy difference calculated from the standard equation between linear ion alignments $P^+B^-P^+$ and $P^+P^+B^-$ is 10 kcal mol^{-1} in the hydrocarbon region if $\epsilon = 2$. This energy barrier is a maximum since co-movement of other ions will reduce it, and the effective dielectric coefficient in a lipid bilayer is greater because of nearby polar regions. Thus the observed extra E_a (~8 kcal mol^{-1}) can be rationalized by the hypothesis of an ion aggregate.

4. The mobility of the cation, much lower than that of the corresponding anion in phosphocholine bilayers, is also enhanced by a factor similar to that which influences the conductivity (Fig. 7). Although this effect could be explained as the canceling of the hypothesized inner positive potential of the bilayer by the negative space charge of borate anions, this explanation fails at low concentrations of borates (Fig. 3). Moreover, the 10-fold shorter transit time of porphyrin cations in the presence of p-$TCPhB^-$ than that in the presence of $TPhB^-$ cannot be expected from this electrostatic effect. The sensitivity of the enhanced mobility of the porphyrin cation to the borate structures is a direct prediction of the ion aggregate model.

5. The following kinetic analysis of the photoinduced current transients strongly supports the dynamic ion chain mechanism. The calculated current traces from this model fit the photoinduced currents very well. The different rate constants of formation, dissociation, and translocation can explain the structural sensitivities.

Kinetic analysis

The photodriven currents in the asymmetric systems are easier for kinetic modeling, because there is no prepolarization caused by outside added voltage, so we mainly consider the kinetics of the asymmetric systems without applied voltage.

A single-site location model of charges in the bilayer has been very useful for electrostatic calculations (McLaughlin, 1989; Mauzerall and Drain, 1992) and for transmembrane kinetics of a single kind of hydrophobic ion (Andersen and Fuchs, 1975; Läuger et al., 1981). In our system, however, the photoformation of P^+ produces strong local fields in the interfacial region and causes rapid short-distance displacements of borate anions. Any unbalanced movements of charge in the bilayer can be recorded as transient electric signals by AC coupling through the "capacitors" of the membrane and its interfaces. These charge displacements must be considered in the analysis of the recorded electric signals. The single-site location model only considers the charge movements across the hydrocarbon core and across the bilayer-water interfaces. Our calculations made with this single-site model cannot fit the two phases of recorded currents (Fig. 7), because the polarization of the photoformed P^+ by B^- anions in the nearby region cannot be considered. A NMR study (Gill et al., 1993) has suggested that there are two binding sites for the borate anions inside the lipid bilayer. Thus, we use the two-site location of free B^- anions in the bilayer shown in Fig. 9. In this model, alternate ion chains across the bilayer are formed by transient binding between photoformed P^+ cations and B^- anions. Both the P^+ cation and the B^- anion have faster

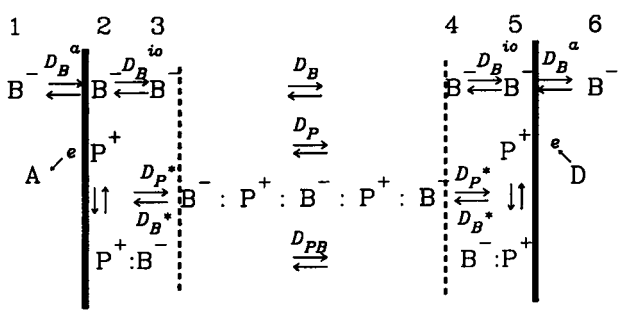

FIGURE 9 Schematic of the two-site location of borate anions inside the bilayer and the dynamic ion-chain model. Positions 1 and 6 represent two aqueous solutions divided by the membrane. Positions 2 and 5 are the outer site of borate anions inside the lipid bilayer. Positions 3 and 4 are the inner site of borate anions. A single site location of P^+ and the ion aggregate is considered to simplify calculations.

translocation rates through the ion chain than by themselves. The total currents are considered as the summation of transmembrane currents of P^+ and B^- and the charge displacement currents (see Appendix). The calculated results from such an ion chain model can fit well the photo-driven current traces for the p-TCPhB$^-$ or p-TFPhB$^-$ system, in both the absence (Fig. 10, *lower dotted curve* versus *solid curve*) and in the presence (Fig. 10, *upper dotted curve versus solid curves*) of a donor. These calculations used identical parameters, except that $k_d = 0$ or $2 \times 10^4\ s^{-1}$. The initial conditions and parameters used for the current calculation (Fig. 10, *dotted curves*) are listed in Table 2. The differences of photoinduced currents between the different borate-porphyrin systems may arise from changes in the association and dissociation rates of the ion chain and the mobilities of the B^- anion and the P^+ cation. For other borate-porphyrin systems, the ion movement currents induced by pulsed light can be similarly fitted by using the ion chain model shown in Fig. 9. This model can also explain the results of Benz (Benz) without having to postulate a membrane crossing time of substituted borates in the ~10-μs time range. The fast relaxation time (μs) can arise from the short-distance movement of ions with little barrier (between sites 2, 3 and 4, 5). The times reported by Benz are in agreement with our observations.

Fig. 11 shows the calculated current components of the p-TCPhB$^-$ system in the absence of donor. The ion displacements coupled through the membrane capacitors cause mainly a current transient on the <1-ms time scale (Fig. 11, *dotted curve*). The positive ionic current on the 1–10-ms time scale mainly arises from the transmembrane diffusion of P^+ cations through the ion chain (Fig. 11, *dotted-dashed curve*). The transmembrane diffusion of B^- anions initially from the opposite side (sites 4, 5 in Fig. 9) toward the P^+ at the acceptor side (site 2) contributes a positive current (Fig. 11, *dashed curve*). In this calculation, we only use the gradient of ion concentration caused by the photogeneration of P^+ and the rapid formation of the neutral ion pair as the driving force of ion movements. The rise time (~0.5 ms) of the transmembrane current components (Fig. 11, *dotted-dashed* and *dashed curves*) is decided by the formation rate constant of the ion chain. The formation of the ion chain is expected to be slower than that of the ion pair, because the alignment of ions takes some time, which possibly decides the rise times of the photogating currents shown in Fig. 2. The dramatic photogating effect of the membrane conductance to borate anions can be explained by translocation of B^- anions hopping along the ion chain with a rate constant $D_B{}^*$. The photogating current traces in Fig. 2 may be fitted using this dynamic ion chain model, but it is more complicated to consider quantitatively the effects of outside added fields on the ion distribution, the ion chain formation, and the ion movements. To make this paper concise, we do not discuss the further complexity of these systems here.

The formation of a variety of organic cation-borate anion complexes in solutions has been reported (Yang et al., 1992; Armitage et al., 1993). One may imagine that a simpler stable aggregate mechanism could explain our results. Suppose that a relatively stable complex between the P^+ cation and the borate anion is formed in the lower dielectric medium of the lipid bilayer. When moving together with the borate anions, P^+ in a complex may show a much higher mobility than the free P^+ cation because of a lower energy barrier. The transmembrane movement of negatively

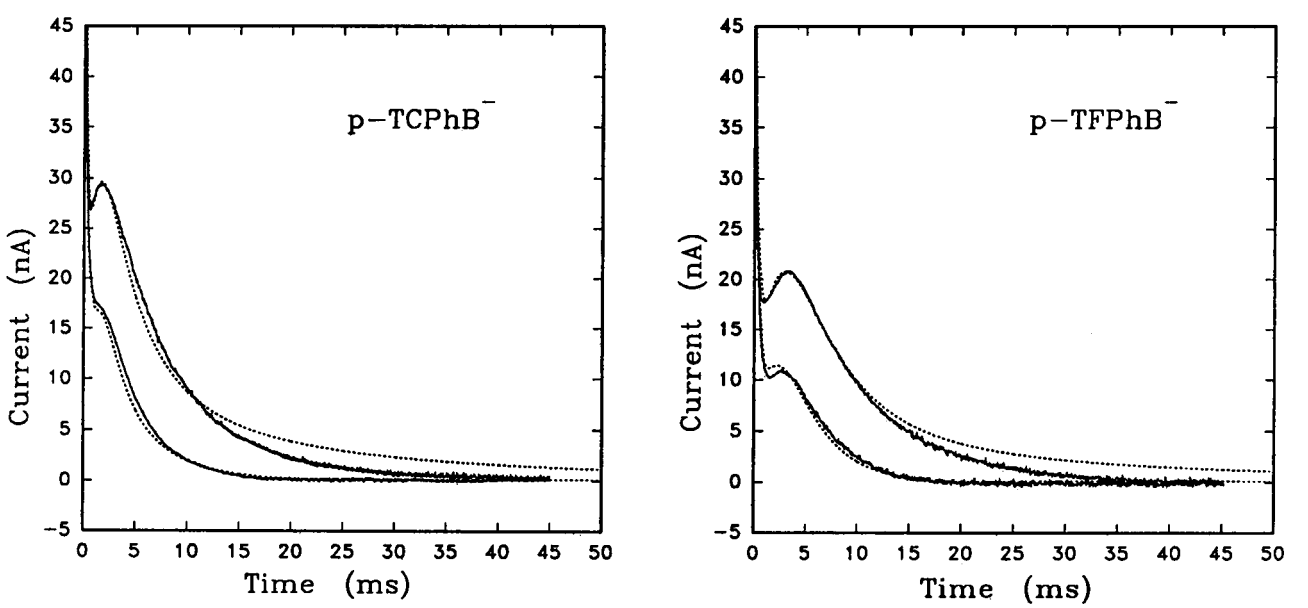

FIGURE 10 The calculated currents from the ion-chain model for the p-TCPhB$^-$ (*left*) and p-TFPhB$^-$ (*right*) systems are plotted together with the measured currents versus time. The lower traces are for the systems without donor. The upper traces are for the systems with donor in the current-saturating concentration. The dotted curves are the calculated currents. The solid curves are the measured current traces for 4 μM borate systems. Parameters are listed in Table 2.

TABLE 2 Parameters used to fit the photodriven currents in Fig. 9 using the dynamic ion chain model

	p-TCPhB$^-$	p-TFPhB$^-$
Initial conditions		
$[P^+]_a^o$ (pmol cm^{-2})	0.16	0.16
$[B^-]_{2,5}^o$ (pmol cm^{-2})	8.0	8.0
$[B^-]_{1,6}^o$ (pmol cm^3)	4.0×10^3	4.0×10^3
β (cm)	2.0×10^{-3}	2.0×10^{-3}
K_b^{io}	0.5	0.5
D_B^a (cm s^{-1})	2.0×10^{-3}	2.0×10^{-3}
D_B (s^{-1})	1.5×10^2	1.2×10^2
D_P (s^{-1})	2.0×10^1	2.0×10^1
k_d (s^{-1})	2×10^4	2×10^4
Variables		
D_B^* (pmol^{-1} cm^2 s^{-1})	6.0×10^4	4.8×10^4
D_P^* (pmol^{-1} cm^2 s^{-1})	1.8×10^4	1.5×10^4
D_B^{io} (s^{-1})	2.0×10^3	1.6×10^3
D_{PB} (s^{-1})	3.3×10^2	3.0×10^2
K_1 (pmol^{-1} cm^2)	2.6×10^{-1}	2.4×10^{-1}
k_2 (pmol^{-3} cm^6 s^{-1})	7.8×10^1	2.6×10^1
k_{-2} (s^{-1})	8.6×10^2	2.9×10^2

$[P^+]^o$ represents the initial concentration of photoformed P^+. $[B^-]_{1,6}^o$ and $[B^-]_{2,5}^o$, respectively, represent the initial concentrations of B^- in aqueous phases and in the membrane interfaces. β represents the partition coefficient of borate anions between the membrane and solution. K_1 represents the formation equilibrium constant of the neutral ion pair P^+:B^-. k_2 and k_{-2} represent formation and dissociation rate constants of the ion chain, respectively. D_B, D_P, and D_{PB} represent the transmembrane diffusion rate constants of free B^-, P^+, and the P^+:B^-. D_P^* and D_B^* represent the diffusion rate constants of P^+ and B^- across the bilayer along the ion chain. D_B^{io} represents the diffusion rate constant of B^- anions from the inner to outer sites (shown in Fig. 8). K_B^{io} represents the equilibrium constant between the inner and outer sites. D_B^a represents the diffusion rate constant of B^- from aqueous phase to the membrane. k_d is the apparent electron transfer rate constant from saturating donor to the transported P^+.

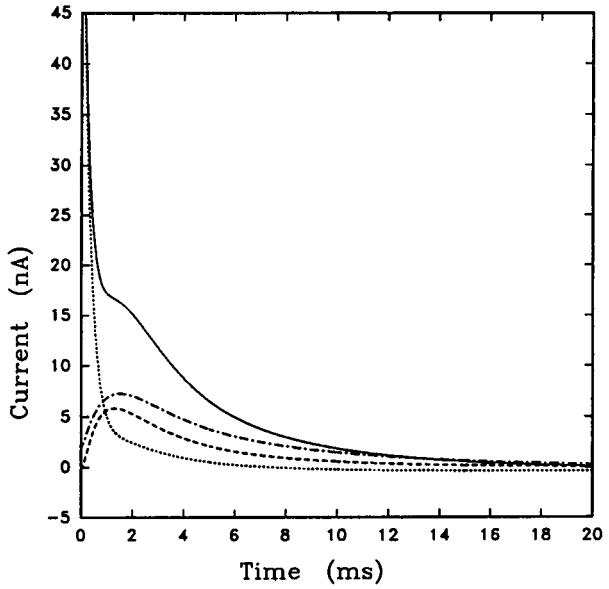

FIGURE 11 The calculated current components of the donor-free membrane system with 4 μM p-TCPhB$^-$ are plotted versus time. The dashed-dotted curve is caused by the transmembrane diffusion of P^+ along the ion chain. The dashed curve is caused by the diffusion of B^- anions along the ion chain. The dotted curve is the current caused by the displacements of B^- anions and coupled through the membrane capacitors. The solid curve is the total calculated current of the system.

charged complexes from the acceptor to opposite sides will cause a negative current. This is contradicted by the observed positive currents (Fig. 7, *A* and *B*). Thus, the positive current may only be caused by the transmembrane diffusion of free borate anions toward the acceptor side. This means that the translocation rate constant of the free borate anion is comparable or even larger than that of the negative complex, which is inconsistent with the large enhanced conductivity. Our kinetic calculations confirm that such a stable complex mechanism cannot explain the results. Thus, our experimental and theoretic results strongly support a dynamic ion chain mechanism.

CONCLUSION

Our results support the view that the hydrophobic anion transport enhanced by the photoformed P^+ cation involves movement of aggregates of these ions. The formation of aggregates also causes ~100-fold enhancement of the translocation rate of P^+ cations and the photodriven P^+-mediated redox flux across the bilayer. The kinetic calculations support a dynamic ion chain mechanism in which both P^+ cations and borate anions can rapidly hop along the ion chain to cross the membrane. This ion effect allows a direct study of ion interactions and electrostatic effects within the bilayer. The photodriven transmembrane charge transfer can be drastically enhanced and controlled by using such an ion-gating effect. This may be helpful in the design of efficient biomimetic and nanoscale molecular devices.

APPENDIX

The scheme for the kinetic modeling using a dynamic ion chain mechanism is shown in Fig. 9. The inner site (position 3 or 4 in Fig. 9) is assumed to have a lower B^- density than the outer site (position 2 or 5 in Fig. 9). We use K_b^{io} to represent the equilibrium constant of the inner to outer sites. The diffusion rate constant of B^- anions between the inner and outer sites (D_B^{io}) is much larger than that across the center of the membrane D_B (Table 1) because of a shorter distance (~10% that of D_B) and a large electrostatic energy at the center.

We suppose that the neutral ion pair P^+:B^- is rapidly formed from B^- anions and P^+ cations after the P^+ is generated (Drain and Mauzerall, 1992) at position 2 in Fig. 9:

$$[P^+:B^-] = K_1[P^+][B^-].$$

K_1 represents the formation equilibrium constant of the neutral ion pair. This depletion of B^- at site 2 causes a fast short-distance movement of B^- from site 3 toward P^+, producing the fast positive current transient. A single-site location (position 2 or 5 in Fig. 9) of free P^+ and the ion pair is considered to simplify the calculations. The specific assumption is that the ion pair can form an ion chain by binding more B^- anions and P^+ cations. The number of P^+ in the bigger aggregate should not be more than that of B^-, to explain the photogating effect of B^- transport (Mauzerall and Drain, 1992). The previous study has suggested that about three B^- anions are involved in the crossing process. About five ions are needed to form the ion chain across the bilayer, considering the thickness of the bilayer and the

size of the ions. Thus we can reasonably express the ion chain as $P_2^+:B_3^-$. The formation of the ion chain is expressed using the following equations:

$$d[P_2^+:B_3^-] = (k_2[P^+:B^-][P^+][B^-]^2 - k_{-2}[P_2^+:B_3^-])dt.$$

k_2 and k_{-2}, respectively, represent the association and dissociation rate constants of the ion chain. The transmembrane translocation rate constants of P^+ cations and B^+ anions along the ion chain are respectively represented by D_P^* and D_B^*. Thus the P^+ and B^- ion fluxes across the middle section of the bilayer from the acceptor to donor sides are expressed as

$$d[P^+]_M/dt = D_P([P^+]_2 - [P^+]_5) + D_P^*[P_2^+:B_3^-]([P^+]_2 - [P^+]_5)$$

$$d[B^-]_M/dt = D_B([B^-]_2 - [B^-]_5) + D_B^*[P_2^+:B_3^-]([B^-]_2 - [B^-]_5).$$

D_P and D_B represent the transmembrane translocation rate constants of the P^+ cation and the B^- anion not in the ion chain, respectively. The total transmembrane current (the movement of negative charge in the D → A direction has a plus sign) is calculated by adding the components across the center of the bilayer:

$$I_M = F(d[P^+]_M/dt - d[B^-]_M/dt).$$

F in the equation is the Faraday constant. However, I_M is not the total current probed from the two electrodes across the bilayer. The transient currents (I_C) caused by the short distance charge displacements can contribute to the total recorded current by AC coupling (polarization) through the membrane capacitors (Hong and Mauzerall, 1976):

$$I_C = F(k_d([P^+B^-]_5 + [P^+]_5) + D_B^{io}([B^-]_3 - K_B^{io}B^-]_2) - D_B^{io}([B^-]_4 - K_B^{io}[B^-]_5) + D_B^a([B^-]_2/0.5\beta - [B^-]_1) - D_B^a([B^-]_5/0.5\beta - [B^-]_6)).$$

k_d represents the rate constant for interfacial electron transfer from the saturating donor to P^+ alone and in the ion pair. D_B^{io} and D_B^a, respectively, represent the translocation rate constants of B^- from the inner to outer sites and from aqueous phases to the outer sites. β is the partition coefficient of B^- in the bilayer to that in aqueous phases. It is multiplied by 0.5 to obtain the concentration of B^- at one membrane interface. In this calculation, the coupling coefficients are considered as 1 for all of the transient current components to simplify the calculation. This does not affect the rationality of the calculation, because the fit of current shape is more significant than that of current amplitudes in such a kinetic analysis. In fact, some terms in the equation only contribute small current components.

The total current probed from aqueous phases through electrodes should be the summation of the transmembrane current and the displacement current coupled through the membrane capacitors:

$$I_T = I_M + I_C.$$

This research was supported by National Institutes of Health grant GM-25693.

REFERENCES

Andersen, O. S., S. Feldberg, H. Nakadomari, S. Levy, and S. McLaughlin. 1978. Electrostatic interactions among hydrophobic ions in lipid bilayer membranes. *Biophys. J.* 21:35–70.

Andersen, O. S., A. Finkelstein, I. Katz, and A. Cass. 1976. Effect of phloretin on the permeability of thin lipid membranes. *J. Gen. Physiol.* 67:749–771.

Andersen, O. S., and M. Fuchs. 1975. Potential energy barriers to ion transport within lipid bilayers. *Biophys. J.* 15:795–830.

Armitage, B., J. Retterer, and D. F. O'Brien. 1993. Dimerization of cyanine dyes in water driven by association with hydrophobic borate anions. *J. Am. Chem. Soc.* 115:10786–10790.

Benz, R. 1988. Structural requirement for the rapid movement of charged molecules across membranes. *Biophys. J.* 54:25–33.

Benz, R., P. Läuger, and K. Janko. 1976. Transport kinetics of hydrophobic ions in lipid bilayer membranes. *Biochim. Biophys. Acta.* 455:701–720.

Cafiso, D. S., and W. L. Hubbell. 1981. EPR determination of membrane potentials. *Annu. Rev. Biophys. Bioeng.* 10:217–244.

Cevc, G. 1990. Membrane electrostatics. *Biochim. Biophys. Acta.* 1031: 311–382.

Chow, H. C., R. Serlin, and C. E. Strouse. 1975. The crystal and molecular structure and absolute configuration of ethyl chlorophyllide a dihydrate. A model for the different spectral forms of chlorophyll a. *J. Am. Chem. Soc.* 97:7230–7237.

DeLevie, 1978. Mathematical modelling δf transport of lipid-soluble ions and ion-carrier complexes through lipid bilayer membranes. *In* Advances in Chemical Physics. I. Prigaogine and S. A. Rice, editors. J. Wiley and Sons, New York. 99–137.

Drain, C. M., B. Christensen, and D. Mauzerall. 1989. Photogating of ionic currents across the lipid bilayer. *Proc. Natl. Acad. Sci. USA.* 86: 6959–6962.

Drain, C. M., and D. Mauzerall. 1992. Photogating of ionic currents across the lipid bilayer: hydrophobic ion conductance by an ion chain mechanism. *Biophys. J.* 63:1556–1563.

Franklin, J. C., and D. S. Cafiso. 1993. Internal electrostatic potentials in bilayers: measuring and controlling dipole potentials in lipid vesicles. *Biophys. J.* 65:289–299.

Fuhrhop, J. H. 1981. Laboratory methods. *In* Porphyrins and Metalloporphyrins. K. M. Smith, editor. Elsevier, New York. 757–869.

Gill, D. J., S. Chandrasekaran, and J. C. Smith. 1993. Location models for potential-sensitive hydrophobic ions, anti-HIV and anti-*Pneumocystis carinii* compounds in model membranes: a NOESY NMR spectroscopy study. *Biophys. J.* 64:A74.

Hong, F. T., and D. Mauzerall. 1976. Tunable voltage clamp method: application to photoelectric effects in pigmented bilayer lipid membranes. *J. Electrochem. Soc.* 123:1317–1324.

Honig, B. H., W. L. Hubbell, and R. F. Flewelling. 1986. Electrostatic interactions in membranes and proteins. *Annu. Rev. Biophys. Biophys. Chem.* 15:163–193.

Huber, H. L., and B. Rumberg. 1981. Determination of potentials and fixed charges and their light-induced changes on the inner surface of the thylakoid membrane. *In* Photosynthesis, Vol. 1. G. Akoyunoglou, editor. Balaban Int. Sci. Serv., Philadephia. 419–429.

Ilani, A., and D. Mauzerall. 1981. The potential span of photoredox reaction of porphyrins and chlorophyll at the lipid bilayer-water interface. *Biophys. J.* 35:79–92.

Jarzembowski, F., F. Cassaretto, H. Posvic, and C. E. Moore. 1974. Studies in tetraarylborates. *Anal. Chim. Acta.* 73:409–412.

Ketterer, B., B. Neumcke, and P. Läuger. 1971. Transport mechanism of hydrophobic ions through lipid bilayer membrane. *J. Membr. Biol.* 5:225–245.

Läuger, P., R. Benz, G. Stark, E. Bamberg, P. C. Jordan, A. Fahr, and W. Brock. 1981. Relaxation studies of ion transport system in lipid bilayer membranes. *Q. Rev. Biophys.* 14:513–598.

Liberman, E. A., and V. P. Topaly. 1969. Permeability of bimolecular phospholipid membranes to lipid-soluble ions. *Biophysics.* 14:477–487.

Mauzerall D., and C. M. Drain. 1992. Photogating of ionic currents across lipid bilayers: electrostatics of ions and dipoles inside the membrane. *Biophys. J.* 63:1544–1555.

McLaughlin, S. 1977. Electrostatic potentials at membrane-solution interfaces. *Curr. Top. Membr. Transp.* 9:71–144.

McLaughlin, S. 1989. The electrostatic properties of membranes. *Annu. Rev. Biophys. Biophys. Chem.* 18:113–136.

Perkins, W. R., and D. S. Cafiso. 1987. A procedure using voltage-sensitive spin labels to monitor dipole potential changes in phospholipid vesicles: the estimation of phloretin-induced conductance changes in vesicles. *J. Membr. Biol.* 96:165–173.

Redwood, W. R., F. R. Pfeiffer, J. A. Weisbach, and T. E. Thompson. 1971. Physical properties of bilayer membranes from a synthetic saturated phospholipid in n-decane. *Biochim. Biophys. Acta.* 233:1–6.

Sun, K., and D. Mauzerall. 1996. Charge transfer across a single lipid-water interface causes ion pumping across the bilayer. *Biophys. J.* 71:3337–3344.

Woodle, M., and D. Mauzerall. 1986. Photoinitiated ion movements in lipid membranes containing magnesium octaethylporphyrin. *Biophys. J.* 50:431–439.

Yang, X., A. Zaitsev, B. Sauerwein, S. Murphy, and G. B. Schuster. 1992. Penetrated ion pairs: photochemistry of cyanine dyes within organic borates. *J. Am. Chem. Soc.* 114:793–794.